

## 0/1 and 3-Dimensional Cold Flow Analysis of a Diesel Engine: A Case Study

Gonca Kethüdaoğlu<sup>1\*</sup> , Fatih Aktaş<sup>2</sup> , Salih Karaaslan<sup>2</sup>  and Nureddin Dinler<sup>2</sup> 

<sup>1</sup>Graduate School of Natural and Applied Sciences, Gazi University, Ankara 06500, Türkiye

<sup>2</sup>Department of Mechanical Engineering, Faculty of Engineering, Gazi University, Ankara 06570, Türkiye

### Abstract

Gas motion in the engine cylinder plays a critical role in diesel engines' air-fuel mixing and combustion processes. Moreover, it influences the engine's performance, emissions, and heat transfer. The intake air motion regulates the main phases of the flow in the cylinder, which is characterized by swirl, squish, and turbulence. Inducing swirl and tumble in the intake process provides high turbulence levels at ignition, resulting in more effective flame speeds and better combustion for lean air-fuel ratios or with EGR. Computational fluid dynamics (CFD) software is used to enhance in-cylinder flow characteristics. In this study, a cold flow simulation of a naturally aspirated, direct injection diesel engine was conducted with different piston bowls using AVL Fire M R2022.2. Swirl, tumble, and TKE parameters were investigated to make a detailed analysis of the in-cylinder flow for the relevant engine. Contrary to the expectation, the swirl ratio for the Piston B configuration is less than that for the original piston configuration. It causes a decrement of swirl ratio compared to the initial piston geometry and the maximum decrement is about 19%. In both cases, the second peak of TKE corresponding to the reverse-squish is around at the -30 CA and the difference between the curves is about  $\pm 8\%$ .

*Keywords:* CFD simulation; Cold flow; Diesel engine; Swirl; Tumble

### Research Article

#### History

Received 01.11.2023  
Revised 30.01.2024  
Accepted 09.02.2024

#### Contact

\* Corresponding author  
[gonca.kethdaoglu@amasya.edu.tr](mailto:gonca.kethdaoglu@amasya.edu.tr)  
Address: Graduate School of  
Natural and Applied Sciences,  
Gazi University, Ankara 06500,  
Türkiye  
Tel: +903122028653

**To cite this paper:** Kethüdaoğlu, G., Aktaş, F., Karaaslan, S., Dinler, N. 0/1 and 3-Dimensional Cold Flow Analysis of a Diesel Engine: A Case Study. International Journal of Automotive Science and Technology. 2024; 8 (1): 142-149. <http://dx.doi.org/10.29228/ijastech.1384376>

### 1. Introduction

Early studies indicated that gas motion in the engine cylinder governs the air-fuel mixing and combustion processes in diesel engines. In addition to this, it affects diesel engine performance and emissions, it also has a considerable effect on engine heat transfer. The intake air motion process controls the main phases of the flow in-cylinder [1,2]. Therefore, in-cylinder air motion during intake stroke was investigated in many studies [3–7]. Air motion is usually defined by swirl, squish, and turbulence for in-cylinder flows. Swirl and tumble are rotational movements, swirl occurs around the cylinder axis, and tumble occurs on an axis perpendicular to the cylinder axis. One of the reasons for inducing swirl and tumble is to provide high turbulence levels at ignition. High turbulence at the ignition process provides more effective flame speeds and better combustion for lean air-fuel ratios or with exhaust gas recirculation (EGR). Under typical air-fuel ratios, the increased flame speed ensures that the flame front reaches the end gas before auto-ignition reactions take place, enabling the potential use of higher compression ratios without the risk of knock [8].

Monaghan and Pettifer conducted a study to investigate the air motion and its effect on diesel performance and emissions. It was indicated that there were differences between the speed responses of the ports and their optimum injection specifications such that

differences in the air motion in the bowl possible effect on engine performance [2]. Prasad et al. presented a study that researched the effect of swirl induced by re-entrant piston bowls on emissions of the diesel engine. Different piston bowls were used in the study, and the best piston bowl geometry for turbulent kinetic energy intensification and swirl about the top dead center (TDC) was investigated. The injection timing of the selected geometry was optimized for the lower NO<sub>x</sub> emission, and 27% NO<sub>x</sub> emissions and 85% soot level reduction were obtained from the baseline configuration [9]. Tsiogkas et al. performed research to increase engine efficiency, the flow field was investigated, and the intake stroke flow was examined using a single-cylinder optical research engine for this purpose. The study was carried out at 1000 and 1500 rpm [10]. The utilization of computer programs in research conducted on vehicles and engines in the literature has been favored due to the benefits they provide [11–13].

Cold flow simulation is utilized to investigate in-cylinder flow characteristics because of the advantages of computational fluid dynamics (CFD). One of the studies conducted using CFD, it was aimed to research the in-cylinder flow characteristics of various piston geometry configurations. The study results showed that although piston geometry configurations had a negligible effect on the intake stroke, they had a considerable effect on the compression stroke, especially near TDC [14]. CFD software is

also used to provide improvement of in-cylinder flow characteristics. Hamid et al. studied to obtain better evaporation for emulsified biofuel with three different piston-bowl geometries. Turbulence kinetic energy (TKE), swirl, and tumble parameters were investigated with cold flow simulation by using Ansys Fluent 15. According to their cold flow simulation results, shallow depth re-entrance combustion chamber (SCC) produced higher swirl, tumble, and regular turbulence flow [15].

Azad et al. investigated that diesel engine cold flow behavior and examined with CFD simulation. In that study, a numerical study conducted using CFD code with k- $\epsilon$  turbulent model. The study reveals the influence of swirl ratio on combustion performance, emissions, and mass-average turbulent kinetic energy higher in exhaust stroke compared to intake stroke. It is stated that further improvement is needed for fuel-efficient diesel engines [16]. Varma and Subbaiah conducted a study to analyze effect of different piston bowl geometries on compression ignition engines. Various piston bowl geometries such as hemispherical combustion chamber (HCC), toroidal combustion chamber (TCC), and shallow depth combustion chamber (SCC) were examined using CFD analysis. The study findings indicate that optimizing the piston bowl geometry can be a beneficial strategy to enhance the air-fuel mixture and decrease emissions in direct injection compression ignition engines [17]. According to the literature review, it can be understood that piston bowl geometry improvement has a potential to enhance the air-fuel mixture and decrease emissions.

This study utilizes AVL Fire M R2022.2 to perform cold flow simulations of a naturally aspirated, direct-injection diesel engine. Then, it investigates the influence of different piston bowl configurations on the in-cylinder flow through cold flow analysis. Swirl, tumble, and TKE parameters are analyzed to gain a comprehensive understanding of the engine's flow characteristics within the cylinder.

## 2. Method

This section discusses the simulations carried out with different mesh densities to ensure precise results, regardless of mesh resolution. It also covers the validation of the model by comparing the computational simulation's results with actual experimental data to ensure the model accurately represents the system's physical behavior. A verification study was conducted using the compression pressure data from Karuk's study [18]. Moreover, the section includes details about the 1D modeling performed with AVL Boost and a comprehensive overview of the computational grids and boundary conditions applied in the 3D cold flow simulation conducted with AVL Fire.

### 2.1. Engine Modelling

The specifications of the engine studied are listed in Table 1. The selected engine is a naturally aspirated, direct-injection diesel engine. The combustion chamber was replaced with a different configuration (referred to as Piston B) since this design was shown to be effective in previous investigations in the literature [19,20].

This configuration was generated based on published literature on diesel engines, and a relative comparison between the two shapes is shown in Figure 1. Piston A represents the standard piston bowl of the engine.

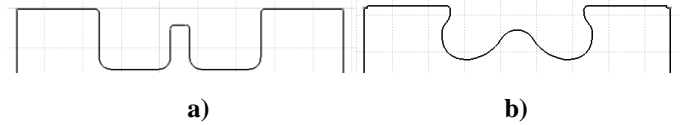


Fig. 1. Piston bowls a) Piston A (standard piston) b) Piston B

Table 1. Engine specifications

Engine type	4-stroke, direct injection diesel engine
Number of cylinders	1
Bore (mm)	85
Stroke (mm)	90
Displacement (cm <sup>3</sup> )	510
Compression ratio	17.5:1
Engine Speed(rpm)	1800

### 2.2. Mesh Independence

Table 2 shows the number of cells for coarse, medium, and fine mesh for the original piston. Figure 2 illustrates the mesh independence test computed for the original piston, where the results are compared in terms of swirl for coarse, medium, and fine mesh.

Table 2. The number of mesh cell

Start Angle- End Angle	Coarse (number of mesh cells)		Medium (number of mesh cells)		Fine (number of mesh cells)	
	min	max	min	max	min	max
EVO(134)- IVO (338)	322347	605241	524611	1009515	913834	1804401
IVO (338)- EVC (389)	331906	653214	530473	1115426	819424	1874589
EVC(389)- IVC (592)	262426	703910	479112	1222945	751118	2192842
IVC (592)- EVO (854)	108577	362486	161199	655716	257975	1207468

In Figure 2, the swirl ratio computed by the Cold Flow simulation shows differences in the data for mesh densities. For fine and medium mesh, the results show that the swirl ratio for these two models is considerably close to each other, with a deviation of about 0.14%.

For the coarse mesh, it can be observed that the deviation of swirl ratio values is around 0.38-3.5% throughout 400-760 CA. In between 330-400 CA, the swirl ratio is -0.070 for coarse and 0.02 for fine mesh at 380 CA with the maximum deviation.

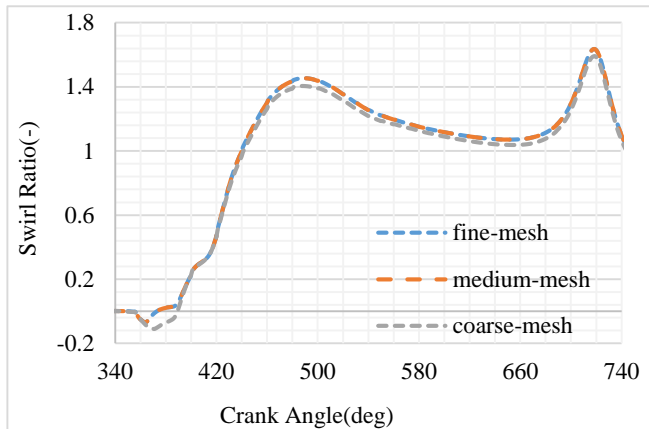


Fig. 2. Swirl ratio for different mesh densities

Fig. 3 illustrates the mesh independence test computed for the original piston, where the results are compared in terms of the TKE for coarse, medium, and fine mesh.

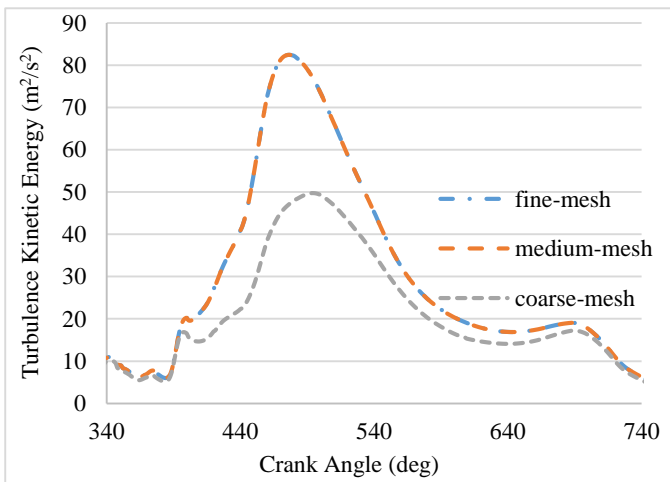


Fig. 3. TKE for different mesh densities

For fine and medium mesh, the results show that the TKE for these two models is close to each other, with a deviation of about 0.029%. For the coarse mesh, it can be observed that the deviation of the TKE values is around 48.63% throughout 330-740 CA. According to the mesh independence test results, the medium mesh is used for all simulations.

## 2.3. Model Verification for Cold Flow

### 2.3.1. AVL Boost- Cold Flow

In previous studies, the engine, whose specifications are given in Table 1, was modeled using AVL Boost R2021.2 software. In this 1-D model, the physical specifications of the engine, boundary conditions at the exhaust valve opening (EVO), heat transfer model, heat transfer surface area, and intake and exhaust valve profiles were defined. Additionally, the model was verified against experimental data from the literature [21]. The experimental study, conducted by Aydın, aimed to investigate the impact of thermal

barrier coating application on the combustion, performance, and emissions of the engine [22,23]. The model was validated using in-cylinder pressure and heat release rate data at 1800 rpm for the standard engine with diesel fuel. It is aimed to verify the model one-dimensionally and to obtain some values that cannot be reached experimentally.

To solve the defined conditions, AVL Boost utilizes basic conservation equations and thermodynamic and heat transfer models. The simulation uses Woschni's 1978 heat transfer model and includes various components of the engine such as connection points, plenum, measurement points, air filter, cylinder, and system boundaries[24]. The cylinder's physical specifications, pressure at EVO, temperature, and heat transfer surface area information, along with intake and exhaust valve details, are defined in the cylinder's submenus[21]. The model, which was previously verified for 1800 rpm, was rearranged for cold flow without any combustion by selecting the "motored" option in the AVL Boost combustion model's section. Cold flow analyses were verified with the measured experimental compression pressure of the relevant engine in the experimental study conducted by Kavruk [18]. In the relevant study, the maximum compression pressure was recorded as  $P_c=45.59$  bar.

The results of the experimental study and the 1D model are consistent, in addition, the difference between the results is about 2.82%. The maximum cylinder pressure is 46.88 for the 1D model. The one-dimensional modeling results show that the volumetric efficiency is about 87%, and the total mass in-cylinder is 506.68 mg at the end of the intake stroke. Figure 5 shows the in-cylinder pressure curves for experimental study and cold flow simulations.

### 2.3.2. AVL Fire – 3D Cold Flow Simulation

AVL FIRE M, CFD software was used to analyze the in-cylinder cold flow processes. This software was validated for engine simulations by researchers [3–7]. The selected engine is a naturally aspirated, direct-injection diesel engine. The engine specifications are given in Table 1. The computational grids of intake stroke (a) and compression stroke (b) are shown in Figure 4. Intake and compression stroke computational grids can be compared according to Figure 1. The intake port is present during the intake stroke; however, it disables after the intake valve is closed. The computation mesh has 1033017 cells at the bottom dead center (BDC) ( $-180^\circ$  CA) and 161199 cells at TDC ( $0^\circ$  CA).

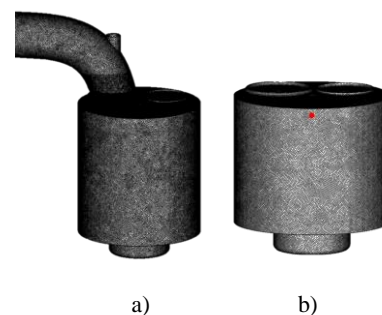


Fig. 4. Computational grid a) intake stroke b) closed part of the cycle.

SIMPLE Based Pressure-Velocity Coupling method is used to link momentum, continuity, and energy equations (coupling between the velocities, pressure, and density) for the solution of the flow field. The  $k - \varepsilon$  model is the most widely used turbulence model for flows, such as those involving heat transfer, combustion, free surface, and two-phase flows. Besides, the  $k - \varepsilon$  provides accurate predictions of main mean-flow properties for most scenarios' situations. For this reason, the  $k - \varepsilon$  model was selected for this cold flow study. The boundary surface and boundary conditions for the model are listed in Table 3. The boundary conditions were determined using experimental data and one-dimensional modeling results. The swirl ratio is assumed as zero for the initial condition of the simulation. As the angular momentum generated by the intake flow greatly exceeds the angular momentum of residual air present at the start of suction, the initial swirl ratio does not have a substantial impact on the outcomes[9].

Table 1. Boundary conditions

Boundary conditions	Momentum boundary condition	Thermal boundary condition
Inlet	Mass Flow	
	Flow direction- Normal to Boundary	
	TKE $1 \text{ m}^2/\text{s}^2$	
	Turbulence length scale 2 mm	
Inlet port Surface	Wall	343.15 K
Outlet	Pressure: 1.15 bar	
Outlet port Surface	Wall	450.15
Head	Wall	423.15 K
Cylinder Wall	Wall	373.15K
Piston top	Wall with mesh movement	443.15 K
Intake Valve surface	Wall with mesh movement	343.15 K
Exhaust Valve Surface	Wall with mesh movement	500.15 K

Cold flow simulation of the engine enables the study of in-cylinder air motion. Studies have shown that for in-cylinder flow calculations for compression, the accuracy of the simulation initial conditions and the flow field values at the end of the intake are significant on predictions at the TDC of compression [25]. Therefore, the whole engine cycle simulation was conducted for cold flow. In the simulation, the intake stroke is between  $-338^\circ$  CA and  $-128^\circ$  CA (considering compression TDC as  $0^\circ$  CA). The closed part of the cycle is between  $-128^\circ$  and  $134^\circ$  CA [26]. During this part of the cycle, the intake port does not include the computational domain.

Figure 5 shows the in-cylinder pressure curves for cold flow. In 3D cold flow analysis, the maximum pressure in the cylinder is 48.53 bar. It was observed that the obtained in-cylinder pressure curve was compatible with the experimental results and the difference for maximum pressure was about 6.4%. The total mass

in-cylinder is 514.35 mg at the end of the intake stroke, the difference with the 1D model is about 1.5%. This provides that the aspirated air mass during intake stroke predicted by simulations is within the acceptable limits [13].

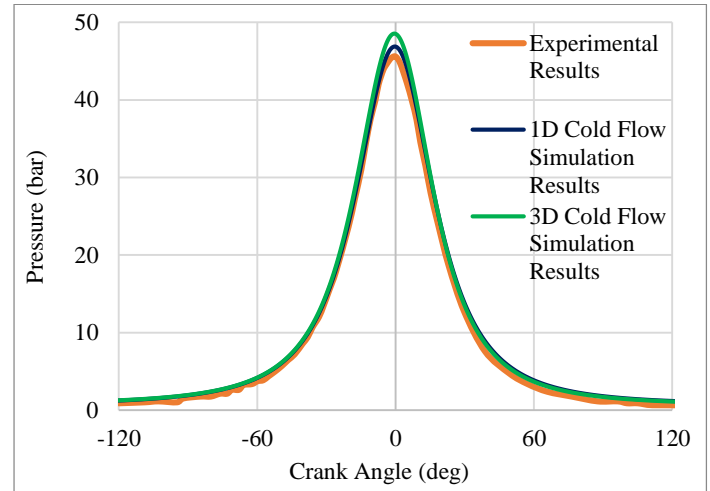


Fig. 5. In-cylinder pressure curves for cold flow

### 3. Results

In this section, the results of the study are presented. After ensuring mesh independence and validation, cold flow analyses were conducted on different piston bowls to assess their effect on cold flow. The parameters that were studied included swirl, tumble, and turbulent kinetic energy.

#### 3.1. Swirl and Tumble

Swirl is a rotational movement that occurs around the cylinder axis. In the study carried out by Crnojevic et al., the swirl movement that occurs due to the movement of the air mass coming from the manifolds into the cylinder was defined analytically and explained with the help of the cylinder of radius [27]  $R$ . The swirl number is the ratio between moments because of the changes in the tangential and axial components of momentum. In addition, it allows the determination of the swirl intensity.

$$S = \frac{M_\varphi}{M_x} = \frac{\int_A (\bar{U}\bar{W} + \overline{u'w'}) r dA}{R \int_A (\bar{U}^2 + \overline{u'^2}) dA} \quad (6)$$

When the velocity terms resulting from the turbulence effect are neglected, the number of swirl intensities according to tangential ( $V_\theta$ ) and axial velocities ( $V_a$ ) is calculated as given in Eq. 7.

$$S = \frac{M_\varphi}{M_x} = \frac{\int_A (\bar{U}\bar{W}) r dA}{R \int_A (\bar{U}^2) dA} \quad (7)$$

Tumble is a rotational movement that occurs on an axis perpendicular to the cylinder axis. The tumble ratio can be defined as the ratio of the equivalent solid-body angular speed by the angular rotation rate of the crankshaft.  $\omega_c$ , the total angular momentum of the charge, is divided by the moment of inertia of the in-cylinder fluid[1].

$$R_t = \frac{\omega_t}{2\pi N} \tag{8}$$

$$R_t = \frac{\int_{\theta_1}^{\theta_2} \rho(r_{xv}) \cdot id\theta}{2\pi N \int_{\theta_1}^{\theta_2} \rho(r \cdot r) d\theta} v \tag{9}$$

### 3.2. Turbulence Kinetic Energy

TKE plays a critical role in internal combustion engines as it influences combustion, mixing, and heat transfer within the engine. Turbulence can significantly affect the combustion process in internal combustion engines, leading to better fuel-air mixing and improved combustion efficiency.

### 3.3. Results of The Cold Flow Simulation

Figure 6 shows the variation of swirl number during the closed part of the cycle. In smaller high-speed diesel engines, swirl ensures faster fuel-air mixing. Swirl is a fluid rotation that occurs around the cylinder axis [1]. At the end of compression, there is a maximum point when the radius of rotation is decreased near TDC. However, the swirl is quickly reduced again during the expansion stroke due to viscous drag with the cylinder walls [18]. Based on the simulation results, the maximum swirl ratio for the closed part of the cycle is 1.63 for Piston A, 1.33, for Piston B at the TDC.

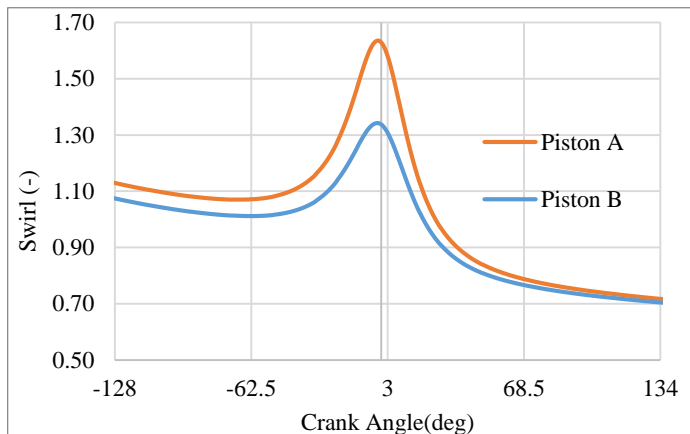


Fig.6 Swirl number for piston bowls

Contrary to the expectation, the swirl ratio for the Piston B configuration is less than that for the original piston configuration. Piston B causes a decrement of swirl ratio compared to the initial piston geometry which is Piston A and the maximum decrement is about 19%. In order to understand this, Fig.7 shows the velocity distributions at different times around TDC for both configurations. Even though two toroidal vortexes form in the combustion chamber due to swirl-squish interaction for Piston B at TDC, it is observed that the maximum velocity in the Piston B configuration is less than the Piston A at all CA in Figure 7. In addition, Distribution of velocity vectors in cylinder's central plane at TDC are shown in Figure 8.

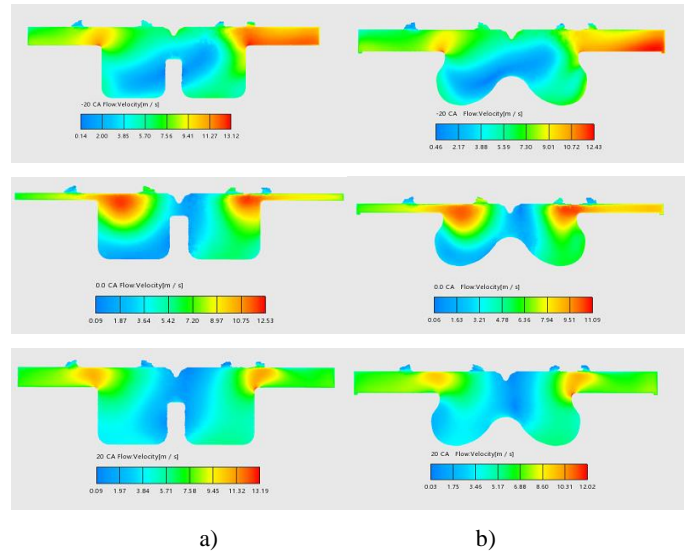


Fig.7. Distribution of velocity in cylinder's central plane a) Piston A (standard piston) b) Piston B

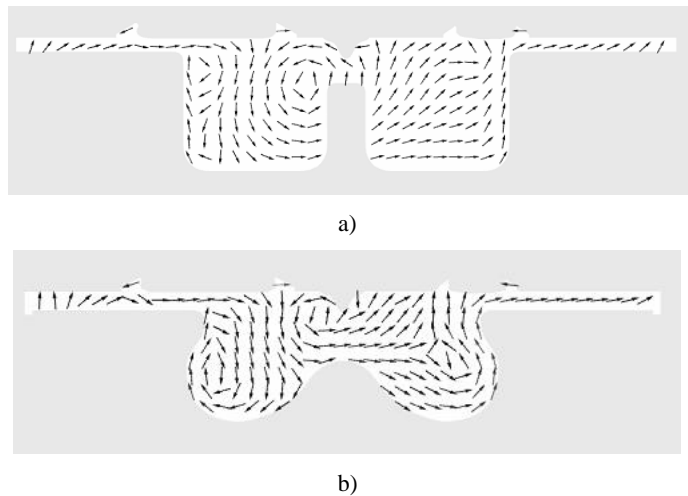


Fig.8. Distribution of velocity vectors in cylinder's central plane at TDC. a) Piston A (standard piston) b) Piston B

Tumble is a fluid motion that occurs on an axis perpendicular to the cylinder axis. As the piston approaches TDC, squish motion produces a secondary rotational flow known as a tumble. When examining the impact of the piston bowl on the tumble ratio, it becomes apparent that, in the case of this specific engine model, the shape of the piston bowl influences the tumble ratio at around the TDC. At TDC, there is a 30.76% difference, with a tumble ratio of -0.13 for Piston A and -0.09 for Piston B (see Figure 9).

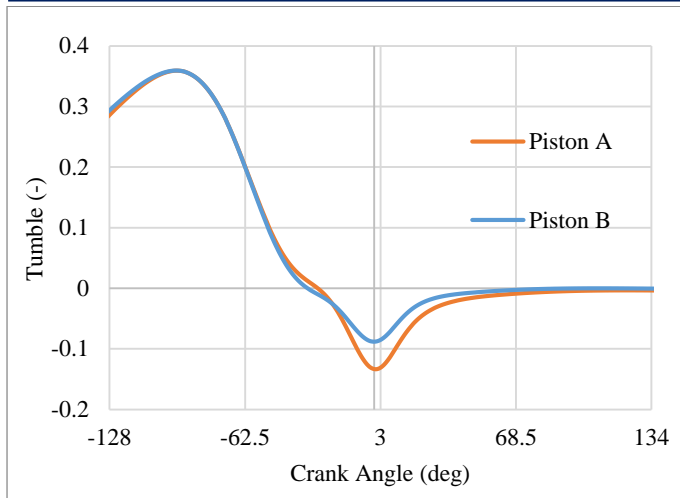


Fig.9. Tumble ratio for piston bowls

The mean TKE variation of the simulation is shown in Figure 10 during the closed part of the cycle. Mean turbulence kinetic energy rises to a maximum because of the high velocities generated during the intake process. Then, it decreases, and this decrease continues during the compression stroke [1]. Turbulence rises once more due to swirl, squish, and tumble near the TDC. The high turbulence near the TDC is asked for better combustion [28]. It can be observed that the TKE values are consistent with the baseline configuration results for Piston B. Both cases exhibit the second peak that corresponds to the reverse squish at around -30 CA. There is a difference of approximately  $\pm 8\%$  between the two curves. The mean value for TKE is  $11.05 \text{ m}^2/\text{s}^2$  for Piston A and  $10.41 \text{ m}^2/\text{s}^2$  for Piston B.

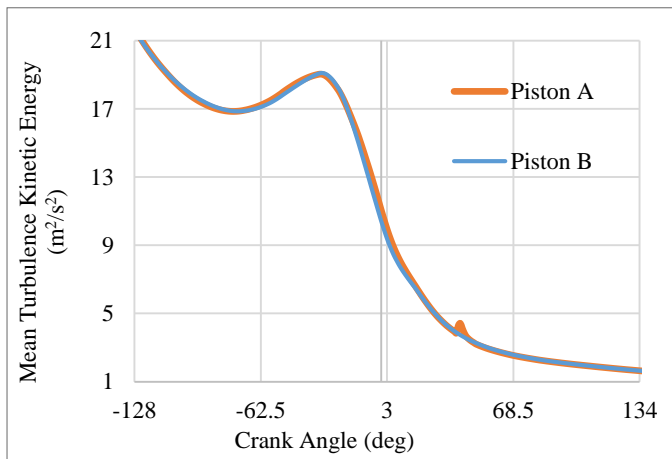


Fig 10. Variation of TKE

The distribution of TKE in the cylinder's central plane is shown in Figure 11. Before TDC, at TDC, and after TDC the maximum values of TKE are slightly higher in Piston B as compared to Piston A. The region with the maximum value of TKE is almost the same in both cases. Thus, from air motion analysis, it can be concluded that the combustion chamber geometry selected from the literature does not provide an improvement for the flow in the present case.

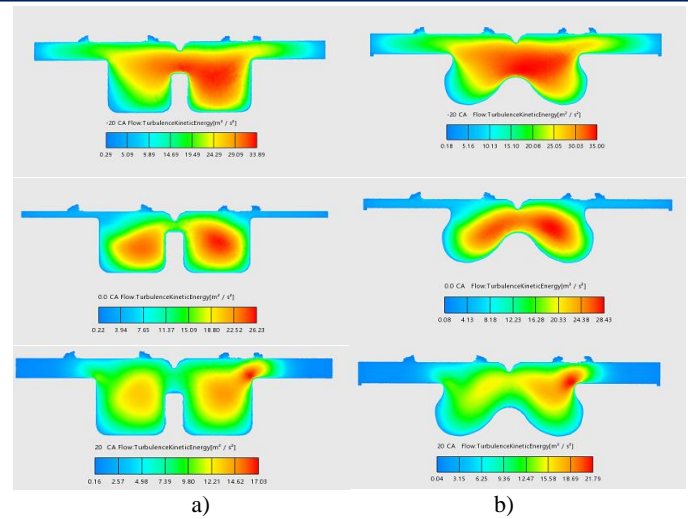


Fig.11. Distribution of TKE in cylinder's central plane. a) Piston A (standard piston) b) Piston B

#### 4. Conclusions

In this study, cold flow simulation of a naturally aspirated, direct injection diesel engine was conducted for different piston bowls by using AVL Fire M. Swirl, tumble, and TKE parameters were investigated.

- The results of the cold flow simulations and experimental results are consistent, the difference between the maximum pressure is about 2.82% for the 1D model and 6.4% for the 3D model.
- The 1-D model volumetric efficiency is about 87%.
- The total mass in-cylinder is 506.68 mg for the 1D model and 514.35 mg for the 3D model at the end of the intake stroke.
- The maximum swirl ratio for the closed part of the cycle is 1.63 for Piston A (standard configuration), 1.33, for Piston B at the TDC.
- The tumble ratio is -0.13 for Piston A (standard configuration) and -0.08 for Piston B at TDC.
- The mean TKE is  $11.05 \text{ m}^2/\text{s}^2$  for Piston A and  $10.41 \text{ m}^2/\text{s}^2$  for Piston B.

According to the conclusions of the study, air motion analysis, it can be concluded that the combustion chamber geometry selected from the literature does not provide an improvement for the flow in the present case. Previous studies have indicated that improving the geometry of the piston has the potential to enhance air-fuel mixing and reduce emissions. Therefore, cold flow simulation studies can be conducted in various bowl geometries to obtain an improvement.

#### Acknowledgment

This study was supported by TUBITAK/TÜRKİYE in the frame of the project code of 122M511 as researchers, we thank the TUBITAK/TÜRKİYE. We would like to express our gratitude to AVL LIST GmbH for providing AVL Boost and FIRE software as part of the University Partnership Program.

## Nomenclature

<i>BDC</i> :	Bottom Dead Center
<i>CFD</i> :	Computational fluid dynamics
<i>EGR</i> :	Exhaust gas recirculation
<i>EVO</i> :	Exhaust valve opening (EVO)
<i>TDC</i> :	Top Dead Center
<i>TKE</i> :	Turbulence Kinetic Energy

## Conflict of Interest Statement

The authors declare that there is no conflict of interest in the study.

## CRediT Author Statement

**Gonca Kethüdaoğlu:** Writing - original draft, Analysis, Validation,

**Fatih Aktaş:** Writing - original draft, Analysis, Validation, Supervision

**Salih Karaaslan:** Writing - review & editing, Supervision

**Nureddin Dinler:** Writing - review & editing, Supervision

## References

- [1] Heywood JB. Internal Combustion Engine Fundamentals. 2nd Edition. McGraw Hill, 2018.
- [2] Monaghan ML, Pettifer HF. Air motion and its effect on diesel performance and emissions. SAE Technical Papers, 1981. <https://doi.org/10.4271/810255>.
- [3] Karami R, Rasul MG, Khan MMK, Mahdi Salahi M. Experimental and computational analysis of combustion characteristics of a diesel engine fueled with diesel-tomato seed oil biodiesel blends. Fuel 2021;285. <https://doi.org/10.1016/j.fuel.2020.119243>.
- [4] Mittal G, Gwalwanshi M. Influence of reentrant piston bowl geometry on combustion in CI engine. Mater Today Proc, vol. 46, 2021. <https://doi.org/10.1016/j.matpr.2021.02.098>.
- [5] Mittal G, Subhash M, Gwalwanshi M. Effect of initial turbulence on combustion with ECFM-3Z model in a CI engine. Mater Today Proc, vol. 46, 2021. <https://doi.org/10.1016/j.matpr.2021.02.097>.
- [6] Hassan NMS, Rasul MG, Harch CA. Modelling and experimental investigation of engine performance and emissions fuelled with biodiesel produced from Australian Beauty Leaf Tree. Fuel 2015; 150:625–35. <https://doi.org/10.1016/J.FUEL.2015.02.016>.
- [7] Soni DK, Gupta R. Numerical analysis of flow dynamics for two piston bowl designs at different spray angles. J Clean Prod 2017; 149:723–34. <https://doi.org/10.1016/J.JCLEPRO.2017.02.142>.
- [8] Lumley JL. Engines: An Introduction. Cambridge University Press; 1999. <https://doi.org/10.1017/CBO9781139175135>.
- [9] Prasad BVVSU, Sharma CS, Anand TNC, Ravikrishna R V. High swirl-inducing piston bowls in small diesel engines for emission reduction. Appl Energy 2011;88. <https://doi.org/10.1016/j.apenergy.2010.12.068>.
- [10] Chraniotis A, Tourlidakis A, Tsiogkas VD, Chraniotis A, Kolokotronis D. Cold Flow Measurement in Optical Internal Combustion Engine using PIV. 13th International Symposium on Particle Image Velocimetry – ISPIV 2019, 2019, München, Germany.
- [11] KIYAKLI AO, SOLMAZ H. Modeling of an Electric Vehicle with MATLAB/Simulink. I Int J Automot Sci Technol. 2018;2. <https://doi.org/10.30939/ijastech..475477>
- [12] Polat S, Yücesu HS, Kannan K, Uyumaz A, Solmaz H. Experimental comparison of different injection timings in an HCCI engine fueled with n-heptane Int J Automot Sci Technol.2017;1.
- [13] Haidar F. Integrated Vehicle Dynamics Modeling, Path Tracking, and Simulation: A MATLAB Implementation Approach. Engineering Perspective 2024;1:7–16.
- [14] Shafie NAM, Said MFM. Cold flow analysis on internal combustion engine with different piston bowl configurations. Journal of Engineering Science and Technology 2017;12.
- [15] Hamid MF, Idroas MY, Sa'ad S, Saiful Bahri AJ, Sharzali CM, Abdullah MK, et al. Numerical investigation of in-cylinder air flow characteristic improvement for Emulsified biofuel (EB) application. Renew Energy 2018;127. <https://doi.org/10.1016/j.renene.2018.04.006>.
- [16] Azad AK, Halder P, Nanthagopal K, Ashok B. Investigation of diesel engine in cylinder flow phenomena using CFD cold flow simulation. Advanced Biofuels: Applications, Technologies and Environmental Sustainability, 2019. <https://doi.org/10.1016/B978-0-08-102791-2.00013-1>.
- [17] Prakash Varma PS, Subbaiah KV. CFD Analysis of piston bowls geometry for CI direct injection engine using finite element analysis. Int J Nonlinear Anal Appl 2022;13.
- [18] Kavruk KÖ. Antor 3ld 510 Dizel Motorunda Mr–1 Yanma Odası Kullanımının Silindir İçi Parametrelere ve Performansa Etkilerinin İncelenmesi[Yüksek Lisans Tezi]. İstanbul Teknik Üniversitesi, 2008.
- [19] Abdelrazek MK, Abdelaal MM, El-Nahas AM. Piston bowl shape and biodiesel fuel effects on combustion and emission of diesel engines. Journal of Engineering and Applied Science 2022;69. <https://doi.org/10.1186/s44147-022-00158-5>.
- [20] Zhang L, Ueda T, Takatsuki T, Yokota K. A study of the effects of chamber geometries on flame behavior in a di diesel engine. SAE Technical Papers, 1995. <https://doi.org/10.4271/952515>.
- [21] Kethudaoglu G, Aktaş F, Karaaslan S, Polat S, Dinler N. Investigation of conversion of a diesel engine to homogeneous charge compression ignition engine using n-heptane: A zero-dimensional modeling. International Journal of Energy Studies. Int J of Energy Studies 2023; 8:3 535 - 556. <https://doi.org/10.58559/IJES.1325924>.
- [22] Aydin S, Sayin C. Impact of thermal barrier coating application on the combustion, performance and emissions of a diesel engine fueled with waste cooking oil biodiesel-diesel blends. Fuel 2014;136. <https://doi.org/10.1016/j.fuel.2014.07.074>.
- [23] Selman Aydın. Yanma Odası Yüzeyleri ZrO<sub>2</sub>, MgO VE Al<sub>2</sub>O<sub>3</sub>[ Doctoral Thesis]. Marmara University, 2014.
- [24] Aktas F. A 0/1-Dimensional Numerical Analysis of Performance and Emission Characteristics of the Conversion of Heavy-Duty Diesel Engine to Spark-Ignition Natural Gas Engine. Int J Automot Sci Technol. 2022;6. <https://doi.org/10.30939/ijastech..980338>
- [25] Stephenson PW, Rutland CJ. Modeling the effects of intake flow characteristics on diesel engine combustion. SAE Technical Papers, 1995. <https://doi.org/10.4271/950282>.

- [26]Karahan Ő. Biodiesel ile alıŐan diesel motorunda ECFM-3Z (extended coherent flame model- 3 zones) modelinin performans ve emisyon simülasyonuna yaklaŐımı [Doctoral Thesis]. Yıldız Teknik University, 2011.
- [27]Crnojevic C, Decool F, Florent P. Swirl measurements in a motor cylinder. Exp Fluids 1999;26. <https://doi.org/10.1007/s003480050321>.
- [28]Pulkrabek WW. Engineering Fundamentals of the Internal Combustion Engine, 2nd Ed. J Eng Gas Turbine Power 2004;126. <https://doi.org/10.1115/1.1669459>.